persion in Crystal Optics and the Theory of Excitons (Interscience, New York, 1966), p. 25.

[22]J. J. Hopfield, in *Quantum Optics*, edited by R. J. Glauber (Academic, New York, 1969), p. 340.

PHYSICAL REVIEW B VOLUME 5, NUMBER 5 1 MARCH 1972

Spin Dynamics in the One-Dimensional Antiferromagnet $(CD_3)_4NMnCl_3$

M. T. Hutchings* and G. Shirane
Brookhaven National Laboratory, † *Upton, Long Island, New York* 11973

and

R. J. Birgeneau‡
Bell Laboratories, Murray Hill, New Jersey 07974

and

S. L. Holt
Chemistry Department, University of Wyoming, Laramie, Wyoming
(Received 9 July 1971)

Recent studies of the instantaneous magnetic correlations in $(CD_3)_4NMnCl_3$ using quasielastic-neutron-scattering techniques have shown that the $MnCl_3$ chains in this compound exhibit purely one-dimensional paramagnetic behavior down to 1.1 °K. The interactions between Mn^{2+} ions along the chain are such that a molecular field theory would predict an ordering at ~76 °K. It was found that both the spatial and thermal variation of the instantaneous correlations could be quantitatively accounted for using Fisher's theory for the classical Heisenberg linear chain. In this paper we report a detailed study of the time-dependent magnetic correlations in $(CD_3)_4NMnCl_3$ using inelastic-neutron-scattering techniques. It is bound that at low temperatures, for $q \gg \kappa$ and $\omega \neq 0$, the Van Hove scattering function $S(\vec{Q}, \omega)$ may be accurately described by spin-wave theory with a dispersion relation $\hbar\omega = 6.1/\sin\pi q_c^z$* meV over the entire one-dimensional Brillouin zone, even though there is no long-range order. As the temperature is increased from 1.9 to 40 °K these "spin waves" typically weaken in intensity and broaden asymmetrically, with the scattering increasing on the low-energy side. In no case were both well-defined spin waves and a central diffusive component observed simultaneously, although the latter, if weak, could have been masked by the large incoherent scattering.

I. INTRODUCTION

Recently, there has been considerable effort on the part of experimentalists and theorists to understand the dynamical behavior of the spins in Heisenberg paramagnets both near T_c and at higher temperatures. The most complete study to date has been on the compound $RbMnF_3$, which is an excellent example of a three-dimensional (3d) Heisenberg antiferromagnet.[1-9] One of the striking features of the spin dynamics near T_N in this system is the persistence of magnonlike modes into the paramagnetic regime.[1] This effect is more pronounced for systems of lower dimensionality, such as the 2d antiferromagnet K_2NiF_4[10] and the linear-chain system $CsMnCl_3 \cdot 2H_2O$.[11] The possible existence of paramagnetic spin waves, together with the fact that a truly 1d system cannot exhibit long-range order at nonzero temperatures,[12] make a complete study of the dynamics of an ideal 1d Heisenberg paramagnet particularly appealing.

In this paper we report a detailed study of the spin dynamics in the linear-chain antiferromagnet $(CD_3)_4NMnCl_3$ (TMMC).[13] Both bulk-susceptibility measurements[14] and measurements of the instantaneous correlations[15] using quasielastic-neutron-scattering techniques have shown that the $MnCl_3$ chains in this material exhibit remarkably good 1d paramagnetic behavior from high temperatures (the molecular-field-ordering temperature T_{MF} is ~76 °K) down to 1.1 °K. Furthermore, the instantaneous correlations can be quantitatively accounted for at all temperatures using Fisher's[16] exact solution for the classical Heisenberg 1d antiferromagnet with nearest-neighbor interactions. The dynamics of the spins in this system therefore should be particularly amenable to theory.

Theoretical work on the spin dynamics of the linear antiferromagnetic chain at other than infinite temperatures has until recently been wholly concerned with the $S = \frac{1}{2}$ case at 0°. Lieb, Schultz, and Mattis[17] derived the spectrum of first excited states for the XY model, and that for the Heisenberg model has been calculated exactly by des Cloizeaux and Pearson.[18] In both cases these states have been identified as magnonlike states with a simple sine dispersion curve, although the coefficients differ for the two models. des Cloizeaux and

Gaudin[19] have extended the latter work, in a less rigorous manner, for general anisotropic Hamiltonians ranging between the XY and Ising limits.

For higher spins and finite temperatures the theoretical work is conspicuous by its absence, and it is therefore clearly of importance to provide experimental data which can guide such theory. Recent work by McClean and Blume,[20] performed in conjunction with the present experiments, has begun to fill this gap. Computer "experiments" by Blume, Watson, and Vineyard[21] on finite linear chains of classical spins also promise to supply useful additional information. Some exact calculations of $\mathcal{S}(\vec{Q}, \omega)_T$ for finite chains of spins with $S = \frac{1}{2}$ have recently been carried out by Richards and Carboni.[22] There has been considerable work on the dynamical behavior of linear chains of spins at infinite temperatures.[23] These calculations indicate that at long wavelengths $\mathcal{S}(\vec{Q}, \omega)$ has a Lorentzian form, but at shorter wavelengths it has a broad profile with a peak at nonzero ω which may be a remnant of the zero-temperature spin-wave-like excitations. Virtually none of the above theoretical calculations, however, have as yet been substantiated by experiment.

The format of the paper is as follows. In Sec. II we describe the crystal preparation and the crystal structure of TMMC. Section III reviews the static magnetic properties including the quasielastic-neutron-scattering results. Section IV gives a brief description of the theory of inelastic scattering as applied to 1d systems. In Sec. V we explain in detail the experimental techniques and the experimental results. Finally in Sec. VI the results are discussed and general conclusions are drawn.

II. CRYSTAL PREPARATION AND STRUCTURE

A. Preparation of TMMC-d_{12}

The single crystals used for the neutron experiments were prepared in the following manner. 19.8 g of reagent-grade $MnCl_2 \cdot 4H_2O$ (Baker and Adamson) was dehydrated and added to a solution of 12.1 g of tetramethyl-d_{12} ammonium chloride (Merck, Sharp, and Dohme) in 50 ml of 2N DCl (diaprep). All solid was dissolved by gently warming. The solution was then placed in a dessicator over P_2O_5. Within 2 days small bright red crystals were observed to have formed. The container was removed from the dessicator and suitable seed crystals extracted from the solution. The solution was then diluted with 2N DCl until the remaining crystals redissolved. Following this, the container was maintained at a temperature of 70 °C and in a humidity of approximately 10%. A period of 2–3 weeks was required after the introduction of a seed crystal to obtain samples of suitable size for neutron-diffraction measurements. Typical crystal habit was a tablet with the long crystal axis being a c crystallographic axis. Mosaic spreads were less than 10 min. The deuteration, which is necessary to minimize incoherent neutron scattering, was ~ 99% complete.

Three samples were used in the experiments, with volumes of 0.1, 0.4, and 0.7 cm^3. The measurements presented here were made mainly on the largest crystal. Orientations were used which enabled the (hhl), ($h0l$), and ($hk0$) peaks, indexed on a hexagonal lattice, to be observed.

B. Room-Temperature Structure

Morosin and Graeber[24] have determined the structure of $(CH_3)_4N\,MnCl_3$ at room temperature using x-ray diffraction. The crystal is hexagonal with lattice constants $a = 9.151$ Å, $c = 6.494$ Å. Our data on the deuterated crystals agree with these values. There is some ambiguity in the exact space group for TMMC. There are a variety of possible models including one in which the space group is $P6_3$ and a second in which it is the centrosymmetric $P6_3/m$. In the former the chlorine atoms are not fixed exactly at $\frac{1}{4}$ of a unit cell along the c axis, but the $(CD_3)_4N^+$ ions are ordered along the threefold axis $\frac{1}{3}$, $\frac{2}{3}$, z. In the second model the chlorines are at exactly $z = \frac{1}{4}$, but the $(CD_3)_4N^+$ ions are statiscally disordered. The differences between these various structures are small and for our purposes not especially important so that we shall simply assume the centrosymmetric structure. As we shall see, this choice is supported by the quasielastic-neutron-scattering results which indicate significant $(CD_3)_4N^+$ disorder. The crystal structure deduced using this model is shown in Fig. 1. From the fig-

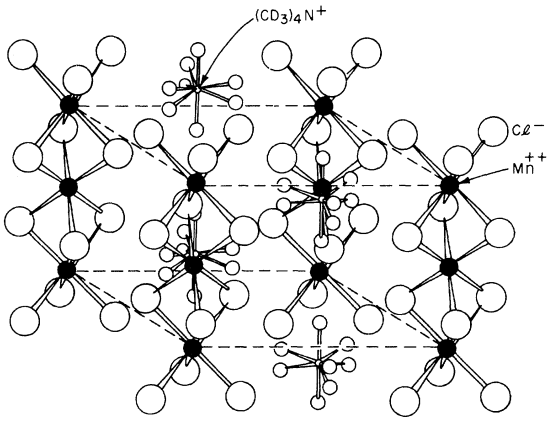

FIG. 1. Crystal structure of $(CD_3)_4NMnCl_3$; this structure is based on the space group $P6_3/m$ with the $(CD_3)_4N^+$ ions statistically disordered relative to the crystal c axis; both possible orientations of these ions are shown. Note that the deuterium ions are not explicitly displayed. Figure adopted from Ref. 24 (Stucky).

ure it may be seen that the compound is composed of infinite $MnCl_3$ chains which are effectively magnetically insulated from each other by the intervening tetramethylammonium ions. The manganese ions occupy special positions at (000) and $(00\frac{1}{2})$ and are surrounded by trigonally distorted octahedra of chlorine ions. Adjacent octahedra share $\{111\}$ faces.

C. Crystallographic Phase Change

On cooling our deuterated samples from room temperature to 78 °K a number of nuclear-diffraction peaks were seen to change markedly in intensity, decreasing by as much as $\frac{1}{80}$. In order to investigate this more closely, the $(500)N$ and $(004)N$ peaks were followed as the temperature was reduced from 150 to 78 °K. The $(500)N$ peak was observed to split at ~128 °K indicating a crystallographic phase change at this temperature. The $(004)N$ reflection, on the other hand, exhibited no anomaly either in intensity or width. The low-temperature phase was not examined in detail, but all the new peaks were consistent with a monoclinic structure with $\gamma = 59.5°$ and the unit cell increasing in length along the smaller axis in the basal plane by a factor of 4. The larger lattice constant in this plane remained close to its room-temperature value. The variation of these lattice constants is shown in Fig. 2. Observation in the $(hk0)$ plane near $(330)N$ showed the presence of at least five of the domains expected from twinning. A weak $(001)N$ peak, forbidden for $P6_3/m$, was observed, and this and a number of very weak extra peaks below 128 °K were attributed to multiple Bragg processes.

As may be seen in Fig. 2, the lattice constant along the unique axis varies smoothly with temperature. In addition, as noted above, none of the $(0\,0\,2n)N$ reflections give any indication of the 128 °K structural transition. It would seem, therefore, that the crystallographic phase change involves a repacking of the $MnCl_3$ chains with no change in their nature. *The* ld *character of the magnetic properties is completely unaffected.* It is probable that the structural transition arises from a freezing out of some of the disorder of the $(CD_3)_4N^+$ ions. This is substantiated by the fact that

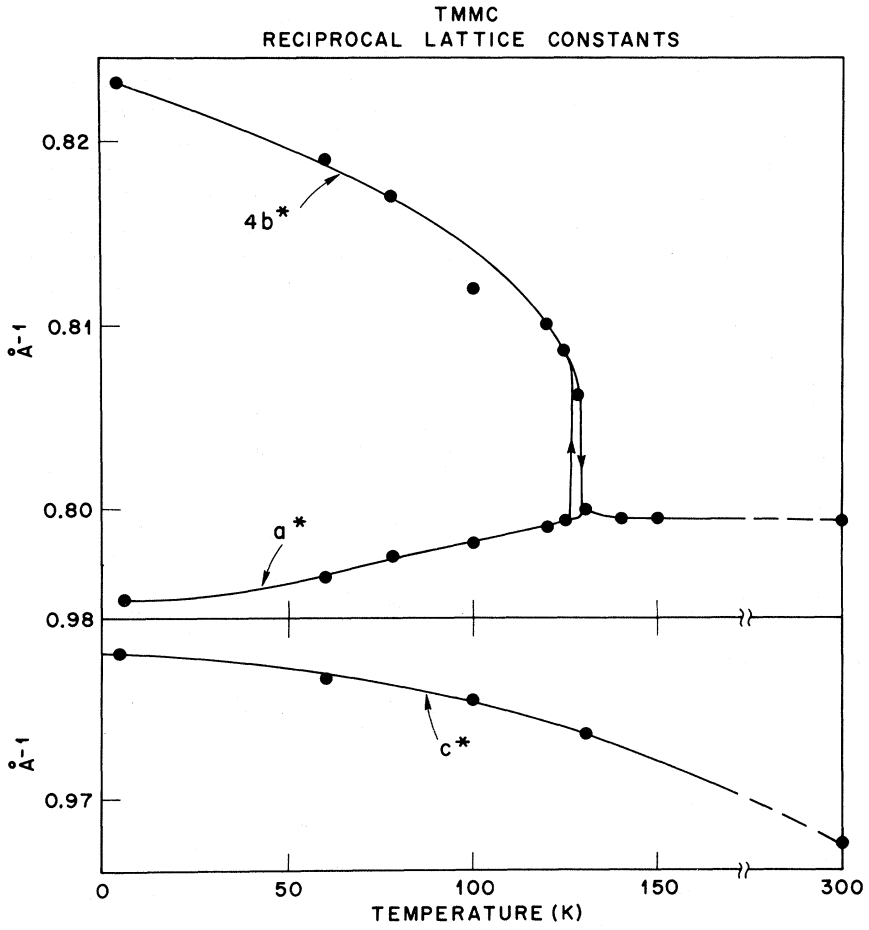

FIG. 2. Lattice constants of TMMC as a function of temperature. The structural phase transition occurs at ~128 °K, below which a^* decreases while b^* is reduced by $\frac{1}{4}$ and increases with decreasing temperature. The hexagonal axis lattice constant c^* is observed to vary smoothly with temperature through the transition.

the incoherent scattering decreased by about a factor of 2 between 140 and 120 °K. In addition, the quasielastic-neutron-scattering experiments[15] showed that there was a strong component in the diffuse scattering arising from molecules aligned in a 1d manner along the c axis but with these chains disordered relative to each other.

For convenience, in this paper we shall refer all reflections to the high-temperature hexagonal axes using c^* and a^* from Fig. 2.

III. STATIC MAGNETIC PROPERTIES

A. Bulk Susceptibility

The first direct experimental evidence for the 1d nature of the magnetism in TMMC came from the bulk-susceptibility measurements of Dingle, Lines, and Holt.[14] They found that the susceptibility exhibits a broad maximum near 55 °K and then decreases somewhat with decreasing temperature in an anisotropic fashion. At somewhat lower temperature (< 10 °K for the magnetic field $\vec{H}$ parallel to the c axis and < 4 °K for $\vec{H} \perp c$) the susceptibility begins to increase again. No evidence was found for a phase transition down to 1.5 °K. This behavior is characteristic of paramagnetic systems in which significant antiferromagnetic correlations have developed without the onset of long-range order. Dingle, Lines, and Holt showed that the susceptibility from 300 to 30 °K could be accurately fitted with Fisher's exact solution for the susceptibility of a classical nearest-neighbor 1d Heisenberg antiferromagnet. Writing the interaction in the form of Eq. (2) below, yields $J_{nn} = -6.3$ °K with $S = \frac{5}{2}$. Measurements of the bulk susceptibility of deuterated TMMC have been performed by Sherwood.[25] As expected, the results are found to be identical, within experimental error, to those for the hydrogeneous material.

In an attempt to obtain a slightly more accurate value for J_{nn}, we have also fitted the high-temperature susceptibility using Rushbrooke and Wood's[26] exact quantum-mechanical series expansion for the $S = \frac{5}{2}$ Heisenberg linear chain. The series contains terms out to $[JS(S+1)/k_BT]^6$, which in this case is adequate to describe the susceptibility down to the maximum at 55 °K. Fits to the data from 300 to 60 °K yield $J_{nn} = (-6.28 \pm 0.11)$ °K in good agreement with the value obtained using the classical model. If one includes only the data between 170 and 60 °K, one obtains $J_{nn} = (-6.47 \pm 0.13)$ °K. We shall use this latter value since the former may be affected somewhat by any temperature dependence in J_{nn}.[27]

There are several additional points of note concerning the bulk susceptibility. First, from the anisotropy of the susceptibility relative to the crystal c axis, Dingle *et al.* conclude that the spin Hamiltonian for the chains also contains a small anisotropy term, probably dipolar in origin, which prefers alignment of the spins perpendicular to the chains. This is confirmed by recent electron-paramagnetic-resonance measurements.[28] Second, Dingle *et al.* explain the upturn in the susceptibility at low temperatures (< 10 °K) on the basis of paramagnetic impurities in the presence of a second phase. Smith and Friedberg[29] have observed a similar effect in the linear-chain system $CsMnCl \cdot 2H_2O$ and they postulate that it may be due to finite chain effects since a chain of length N, where N is odd, will follow a Curie-law susceptibility at low temperatures with moment $g\mu_B S$. A simple calculation for TMMC shows that if all of the extra susceptibility observed at lower temperatures were due to finite chain effects, then the average chain would be about 300 spins long. This, in fact, represents a lower limit. Third, Dingle *et al.* also observe a change in $d\chi/dT$ vs T at 0.84 °K which they attribute to the onset of 3d long-range order. This is somewhat indefinite, however, due to the dominance of impurity effects at that temperature. Finally, the extraordinarily good 1d behavior which TMMC exhibits seems to be due to the fact that there is no superexchange between the chains and the interchain-dipolar field is only about 1×10^{-3} °K.

B. Instantaneous Correlations

Although the bulk susceptibility gives a good indication that TMMC is 1d down to 1.5 °K, the true nature of the correlations can only be completely elucidated by direct neutron-scattering measurements. Using the general scattering formulas, Eqs. (5)–(7) below, the cross section for scattering in the quasielastic approximation is given by

$$\frac{d\sigma}{d\Omega_f}(\vec{Q}) \propto S(\vec{Q}) = \sum_{\vec{r}} e^{i\vec{Q}\cdot\vec{r}} \langle \vec{S}_0(0) \cdot \vec{S}_{\vec{r}}(0) \rangle \,. \tag{1}$$

Fisher[16] has shown that for a classical nearest-neighbor Heisenberg linear chain with

$$\mathcal{H} = -2J_{nn} \sum_i \vec{S}_i \cdot \vec{S}_{i+1} \tag{2}$$

the instantaneous correlations are given by

$$\langle \vec{S}_i \cdot \vec{S}_{i+n} \rangle = u^{|n|} S(S+1) \,, \tag{3}$$

where $u = \coth K - 1/K$ with

$$K = 2J_{nn} S(S+1)/k_B T \,.$$

The factor $S(S+1)$, rather than S^2, corrects the expressions to $O(1/S)$ for finite spins. Substitution from Eq. (3) into Eq. (1) yields

$$S(\vec{Q}) = \frac{B}{\kappa^2 + (2/\pi^2)(\cos \pi Q^z + 1)} \,, \tag{4}$$

where

$$\kappa = (1+u)/\pi(-u)^{1/2} \,, \quad B = [(u^2-1)/\pi^2 u] S(S+1) \,.$$

In the above we have written Q^{ℓ} and κ in units of $2\pi/2a$, with $a=\frac{1}{2}c$, the nearest-neighbor separation along the chain. Inspection of Eq. (4) shows that the classical model predicts that there will be *planes* of critical scattering which have minima at even integer Q^{ℓ} and maxima at odd integer Q^{ℓ}. This is illustrated in Fig. 3 which gives the reciprocal lattice appropriate to an $(h0l)$ orientation of TMMC.

In a previous publication[15] we have reported detailed measurements of $d\sigma/d\Omega_f$ in TMMC. The results may be summarized as follows. It is found that there are indeed *planes* of scattering perpendicular to the $MnCl_3$ chain axis from above 40 °K down to 1.1 °K. The planar scattering is found to have two major components, a nuclear contribution which occurs at both even and odd integer Q^{ℓ} and a magnetic contribution which occurs only around odd integer Q^{ℓ}. These two components could be readily separated and the magnetic part could be fitted to Eq. (4) convoluted with the instrumental resolution function to yield κ and B as a function of temperature. The results of these fits are shown in Fig. 4. Both κ and κ^2/B are indeed observed to extrapolate to zero at 0 °K as expected for a 1d system. The solid line in the lower part of Fig. 4 represents the best fit to the experimental results of the classical expression for κ given in Eq. (4), giving $J_{nn} = (-7.7 \pm 0.3)$ °K. The corresponding prediction of the classical model for $(d\sigma/d\Omega_f)_{q=0}^{-1} = \kappa^2/B$ is shown as the solid line in the upper part of the figure. Here one over-all scaling factor is adjusted to give the best fit and again the agreement is excellent. These results may be stated as follows: *Fisher's solution for the classical nearest-neighbor Heisenberg model correctly predicts both the spatial and thermal variation of the instantaneous correlations in* TMMC *at all temperatures between* 40 *and* 1.1 °K.

C. Summary of Static Properties

Both the bulk-susceptibility and the quasielastic-neutron-scattering measurements thus show that TMMC is an almost ideal physical realization of the nearest-neighbor Heisenberg 1d antiferromagnet.

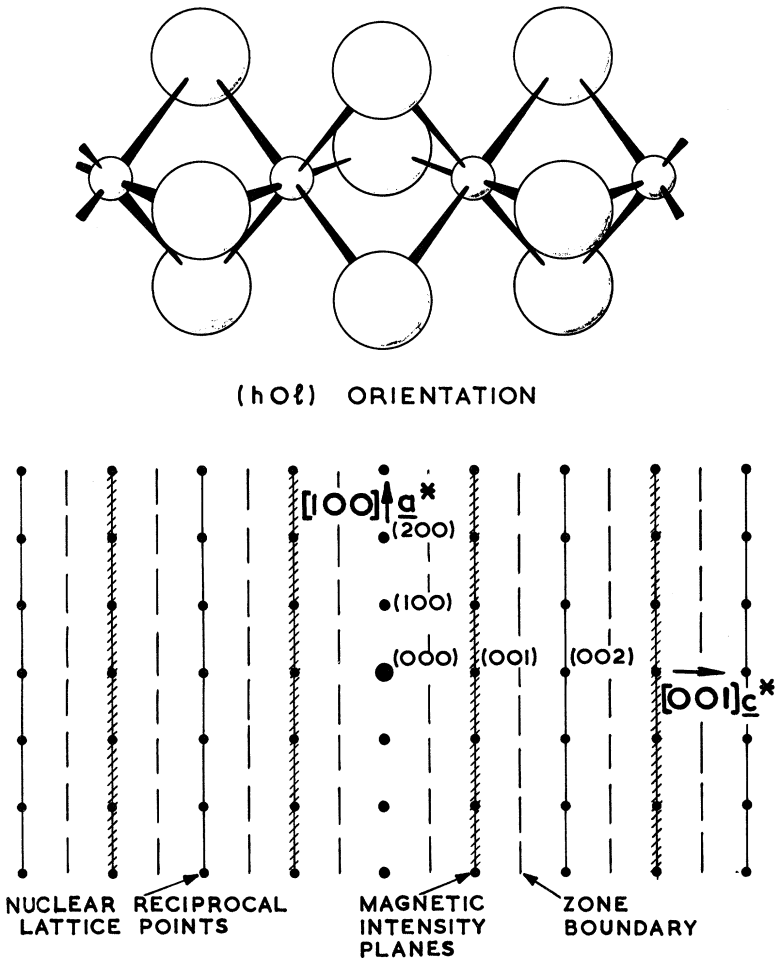

FIG. 3. Top: Magnetic chain part of the TMMC structure. Bottom: The $(h01)$ plane of the reciprocal lattice, used for most of the experiments. The shaded areas denote the positions of these maxima for the planes of magnetic scattering.

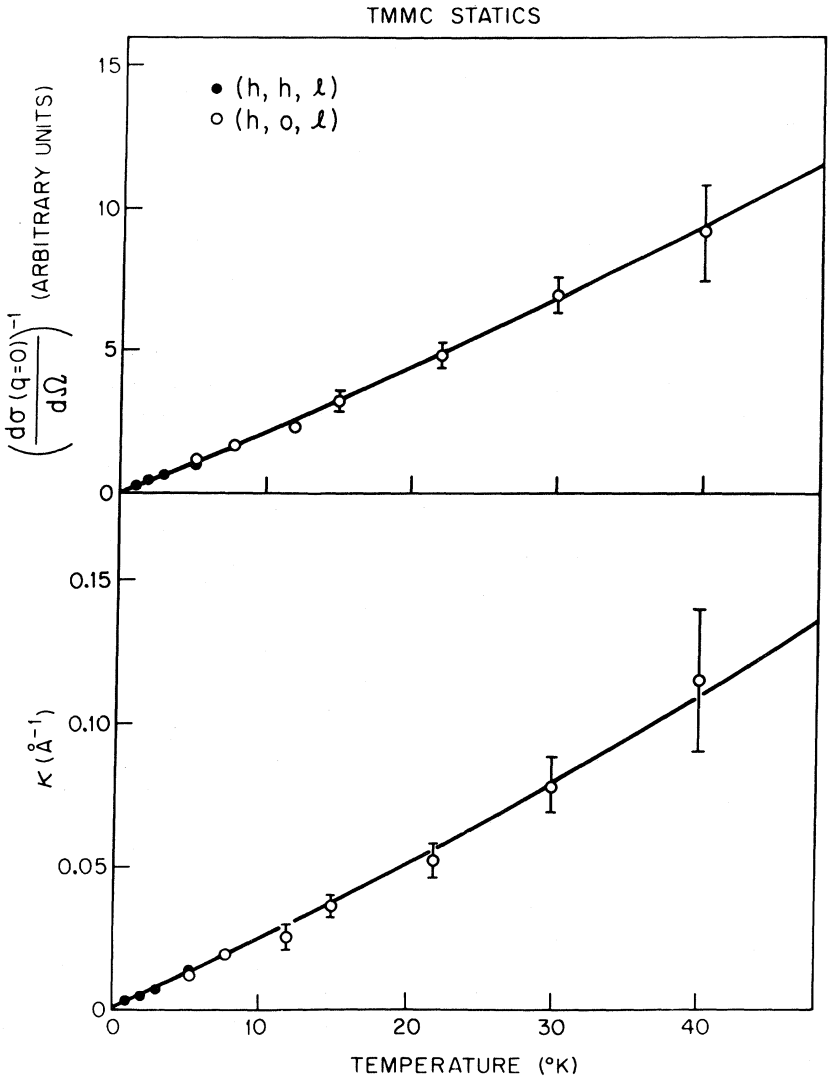

FIG. 4. Inverse correlation length κ in Å^{-1}, and deconvoluted inverse peak intensity $(d\sigma/d\Omega_f)^{-1} = \kappa^2/B$ in TMMC. The solid lines are fits to the classical theory as described in the text. Data taken from Ref. 15.

There is a small anisotropy term of the XY form which manifests itself in the bulk susceptibility but not apparently in the staggered susceptibility. The system is definitely quantum mechanical in the sense that the spin is finite, $S = \frac{5}{2}$, but this does *not* appear to be important in the region $q_{c^*} \lesssim 3\kappa$, where a classical model gives a correct description of $s(q_{c^*})$.

We shall now proceed to discuss the dynamics in this system.

IV. INELASTIC-SCATTERING THEORY

The theory of magnetic neutron scattering in localized paramagnets has been discussed extensively by Marshall and Lowde.[30]

The cross section for scattering of unpolarized neutrons from a system of N localized spins is given by

$$\frac{\partial^2\sigma}{\partial\Omega\,\partial E'} = A(\vec{k}, \vec{k}') \sum_{\alpha\beta} (\delta_{\alpha\beta} - \hat{Q}^\alpha \hat{Q}^\beta)\, s^{\alpha\beta}(\vec{Q}, \omega)\,, \tag{5}$$

where

$$\hbar\omega = E - E' = (\hbar^2/2m)(k^2 - k'^2)$$

and $\hbar\vec{Q} = \hbar(\vec{k} - \vec{k}')$ are the neutron energy and momentum loss, respectively, and

$$A(\vec{k}, \vec{k}') = (N/\hbar)(r_0\gamma)^2 (k'/k)\, |f(\vec{Q})|^2\,; \tag{6}$$

$r_0 = e^2/mc^2$, γ is the neutron gyromatic ratio, and $f(\vec{Q})$ is the magnetic form factor for the spins. The Van Hove scattering function is given by

$$s^{\alpha\beta}(\vec{Q}, \omega) = \frac{1}{2\pi} \sum_{\vec{r}} \int_{-\infty}^{\infty} e^{i(\vec{Q}\cdot\vec{r} - \omega t)} \langle S_0^\alpha(0)\, S_{\vec{r}}^\beta(t)\rangle\, dt\,. \tag{7}$$

The neutron scattering therefore measures directly the space-time Fourier transform of the unequal-time two-spin correlation function. For Heisenberg systems with uniaxial or no anisotropy, $\mathcal{S}^{\alpha\beta}$ vanishes for $\alpha \neq \beta$. In ordered magnetic systems, Eq. (7) can be separated into two parts, a long-range-ordered component obtained from the term $\langle S_0^{\alpha}(0)\rangle\langle S_{\vec{r}}^{\beta}(t)\rangle$, and a fluctuating component arising from $\langle \delta S_0^{\alpha}(0)\, \delta S_{\vec{r}}^{\beta}(t)\rangle$, where $\delta S_{\vec{r}}^{\beta}(t) = S_{\vec{r}}^{\beta}(t) - \langle S_{\vec{r}}^{\beta}(t)\rangle$. However, in a true 1d system there can be no long-range order except at $T = 0\,^{\circ}\mathrm{K}$; that is, $\langle S_{\vec{r}}^{\beta}(t)\rangle = 0$ for $T \neq 0$, so that we may simply use Eq. (7) for the diffuse scattering.

The fundamental problem of spin dynamics in paramagnets, of course, reduces to that of understanding both the spatial and temporal variation of the correlations $\langle S_0^{\alpha}(0) S_{\vec{r}}^{\beta}(t)\rangle$, or equivalently, their Fourier transform $\mathcal{S}^{\alpha\beta}(\vec{Q}, \omega)$. As we have noted in Sec. I, there is at present no theory for $\mathcal{S}^{\alpha\beta}(\vec{Q}, \omega)$ at finite temperatures in a 1d system. Exact calculations by des Cloizeaux and Pearson for the $S = \frac{1}{2}$ 1d Heisenberg antiferromagnet at $T = 0\,^{\circ}\mathrm{K}$ indicate that the first excited states have a spin-wave-like dispersion relation; however, the authors do not calculate the form of $\mathcal{S}(\vec{Q}, \omega)$ itself. In anticipation of our experimental results, it is of interest to calculate $\mathcal{S}(\vec{Q}, \omega)$ within the context of Anderson's two-sublattice spin-wave theory.[31]

Linear-spin-wave theory assumes that the system has long-range order with staggered magnetization proportional to $|\langle S_z\rangle| \simeq S$, where z is the spin direction, and considers small deviations from the Néel ground state. At first sight this would seem to be a very poor approximation to TMMC above $1.1\,^{\circ}\mathrm{K}$ since we know that at these temperatures the system is a 1d paramagnet. Nevertheless, as we shall see, the results turn out to be of considerable value in representing our data. We write the exchange Hamiltonian as in Eq. (2) and include both nearest-neighbor (J_{nn}) and next-nearest-neighbor (J_{nnn}) interactions along the chain, but we ignore all interchain effects. In addition, we shall assume $J_{\mathrm{nn}} \gg J_{\mathrm{nnn}}$. The nearest-neighbor spins, coupled by J_{nn}, are a distance $\frac{1}{2}c$ apart while the next nearest neighbors are c apart. In an ordered antiferromagnet, if z is the spin direction, then the single-spin-wave excitations are associated with the fluctuations transverse to z. It is straightforward to show using standard techniques[32,33] that the spin-wave contribution to $\mathcal{S}^{xx}$, $\mathcal{S}^{yy}$ is given by

$$\begin{Bmatrix} \mathcal{S}^{xx}(\vec{Q}, \omega) \\ \mathcal{S}^{yy}(\vec{Q}, \omega) \end{Bmatrix} = M(q_{c^*})\,[n(q_{c^*}) + \tfrac{1}{2} \pm \tfrac{1}{2}] \times \delta\,(E - E' \mp \hbar\omega(q_{c^*}))\,, \qquad (8)$$

where the amplitude factor, with $J_{\mathrm{nnn}} = 0$, is given by

$$M(q_{c^*}) = (1 - \cos \pi q_{c^*} \cos l\pi)/\sin|\pi q_{c^*}| \qquad (9)$$

and

$$q_{c^*} = Q_{c^*} - l\,.$$

The boson population factor

$$n(q_{c^*}) = \{\exp[\hbar\omega(q_{c^*})/k_B T] - 1\}^{-1}\,, \qquad (10)$$

and the dispersion relation is given by

$$E(q_{c^*}) = \hbar\omega(q_{c^*}) = -R \times 4S\,(J_{\mathrm{nn}} - 2J_{\mathrm{nnn}})\,|\sin \pi q_{c^*}|\,, \qquad (11)$$

where R is a renormalization factor incorporating higher-order corrections to the spin-wave theory.

In the above equations we have written the momenta coordinates along the chain, Q_{c^*}, q_{c^*}, in units of $2\pi/c$. From Eq. (9) it is evident that the intensity should be greatest near the odd-l planes in reciprocal space. It is at these same planes that the intense quasielastic scattering is observed.

The form of the dispersion relation, Eq. (11), indicates that it is not possible to obtain a separate value for J_{nnn} if $|J_{\mathrm{nn}}| \gg |J_{\mathrm{nnn}}|$ and, in fact, we shall assume that J_{nnn} is negligible. The normalization factor R is unity for Anderson's noninteracting spin-wave theory at zero temperature. Oguchi[34] has given the correction factor if the next term of higher order in the spin-wave operators is included. In this case $R = (1 + \epsilon_0/2\eta S)$, where η is the number of nearest neighbors and ϵ_0 involves a summation over the Brillouin zone. For a 1d antiferromagnet, Oguchi's theory gives $\epsilon_0 = 0.726$. Davis[35] has also calculated ϵ_0; using a linked-cluster expansion he finds $\epsilon_0 = 0.665$. Weng and Griffiths[36] have recently proposed an interpolation formula which suggests $R = 1.085$ for $S = \frac{5}{2}$, close to the value of 1.07 given by Oguchi and Davis's theory.

The longitudinal-response function $\mathcal{S}^{zz}(Q, \omega)$ may also be calculated in the spin-wave approximation.[37] In 3d antiferromagnets it is characterized by a broad band originating in two spin-wave-scattering processes. However, in 1d, $\mathcal{S}^{zz}$ (spin wave) is somewhat more complicated and, in particular, in the noninteracting approximation it exhibits a logarithmic singularity at the single-spin-wave position. The singularity occurs because it becomes infinitely easy to create pairs of magnons, one at $(q_{c^*}, \omega(q_{c^*}))$ and the other at $((q_{c^*} \to 0), \omega(q_{c^*} \to 0))$. This feature of the 1d spin-wave theory, however, requires a much more careful treatment than we can give it here. In particular, both magnon-magnon interactions and the thermal modification of the long-wavelength excitations will undoubtedly alter markedly the singularity predicted by the simple theory. Another contribution to $\mathcal{S}^{zz}(\vec{Q}, \omega)$ will be that from bound two-magnon states, which are predicted to play an important role in 1d.[18,38]

The factor $\sum_{\alpha\beta}(\delta^{\alpha\beta} - \hat{Q}^{\alpha}\hat{Q}^{\beta})$ in the scattering cross

section, Eq. (5), has the effect that only the components of $S^{\alpha\alpha}(\vec{Q}, \omega)$ perpendicular to the scattering vector $\vec{Q}$ are observed. In uniaxial antiferromagnets such as MnF_2 it has proved possible to use this feature to demonstrate that the spin-wave scattering is associated exclusively with the components of $S^{\alpha\alpha}(\vec{Q}, \omega)$ perpendicular to the anisotropy axis, even in the paramagnetic regime.[39] In a Heisenberg paramagnet no such separation is possible. In TMMC there is a small (~1%) anistropy of the XY type, that is the spins prefer to be in the plane perpendicular to the $MnCl_3$ chains. It is of interest, therefore, to see if the response function $S(\vec{Q}, \omega)$ displays the same symmetry.

V. EXPERIMENT

A. Experimental Technique; Resolution Corrections

The experimental techniques used were the standard procedures at the Brookhaven H. F. B. R. The samples were mounted on an aluminum pedestal using Hysol-Epoxy-type 1c and sealed in aluminum cans in an atmosphere of helium gas. The Epoxy and pedestal were carefully shielded with cadmium. The cans were mounted in a Cryogenic Associates Dewar type CT14. Their temperature was capable of being controlled between 1.1 and 300 °K, and was measured with either a germanium or platinum resistance thermometer.

The nuclear-diffraction investigations, discussed in Sec. II C, were mainly carried out on the H4S two-axis spectrometer, using neutrons with wavelength $\lambda = 1.03$ Å, energy 77 meV, from a Ge (311) monochromator plane which minimized $\frac{1}{2}\lambda$ effects. 20-min collimation before the monochromator was used, and 10 min before and after the sample. Careful masking was necessary in all experiments in order to reduce the incoherent background to a minimum.

The inelastic measurements were made mainly on the H7 triple-axis spectrometer with incident wavelength of 1.47 Å (38 meV), 2.35 Å (14.8 meV), and 3.89 Å (5.4 meV). Pyrolytic graphite (002) planes were used for both monochromator and analyzer. The monochromator crystal was bent about a horizontal axis to provide a focusing of the incident neutrons.[40] A large mosaic pyrolytic graphite crystal placed before the sample acted as a tuned $\frac{1}{2}\lambda$ filter[41] at the lower two energies. Collimation before and after the sample was kept at 20 min and 40 min respectively, and the in-pile and analyzer-counter collimation was 20 min for the higher incident energies and 40 min for 5.4 meV. As the scattering cross sections were independent of the vertical collimation, this was kept as loose as possible, being mainly determined by the sample height.

In any detailed comparison of experiment and theory it is necessary to take into account explicitly the resolution function of the instrument. When the spectrometer is set to observe the scattering at momentum and energy transfers $(\vec{Q}_0, \omega_0)$, the actual observed intensity is given by the convolution

$$I(\vec{Q}_0, \omega_0) = \int R(\vec{Q} - \vec{Q}_0, \omega - \omega_0)\, \sigma'(\vec{Q}, \omega)\, d\vec{Q}\, d\omega \,. \tag{12}$$

Here R is the instrumental resolution function, which can be represented by the analytic form $R(\vec{x}) = R_0 \exp(-\frac{1}{2}\vec{x}\cdot\vec{\vec{M}}\cdot\vec{x})$, where $\vec{x}$ is the four-component vector (Q^x, Q^y, Q^z, ω), $\vec{\vec{M}}$ is the resolution matrix,[42] and R_0 is a known smoothly varying function of $\vec{k}$ and $\vec{k}'$. σ' is the intrinsic scattering cross section convoluted with the sample mosaic. The components of $\vec{\vec{M}}$ may be calculated from the known instrumental parameters or may be measured experimentally using a nuclear Bragg peak close to the observation position in reciprocal space. In the latter method any effects from sample mosaic are automatically included in R.

In general, deconvolution of the experimental data is not possible unless the explicit analytic form for $\sigma(\vec{Q}, \omega)$ is known. In our case, no such theory is

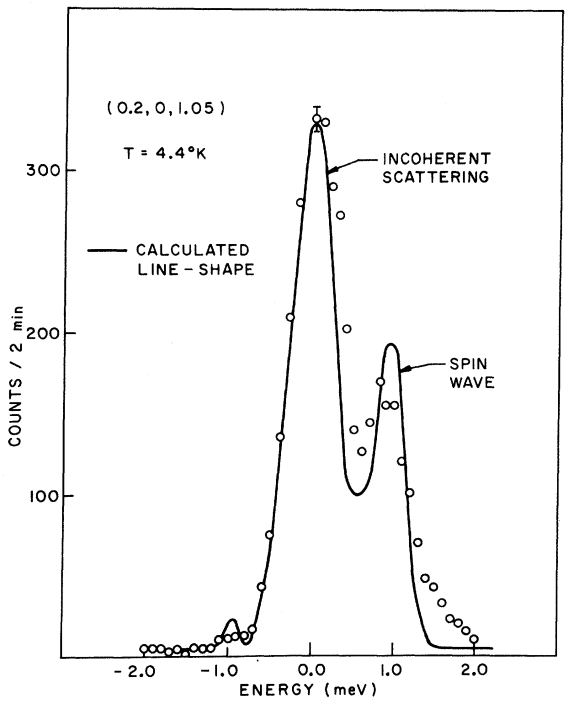

FIG. 5. Constant-Q scan in the position (0.2, 0, 1.05) corresponding to $q_c* = 0.05$ in units of $2\pi/c$. The solid line is the calculated line shape assuming sharp spin-wave scattering and nuclear-incoherent-scattering alone. Note that the observed spin waves are broader than the instrumental resolution function but that the integrated intensities match properly.

available, except at low temperatures where the experimental data suggest that the spin-wave theory discussed in Sec. IV might be valid. In this case, explicit comparisons could be made by numerically convoluting $R(\vec{x})$ with the δ-function cross section for spin-wave scattering, Eq. (9). This was actually carried out using a modified version of the program written by Hutchings and Samuelson.[43] The program includes in R_0 the variation of monitor, analyzer, and counter efficiency with energy to an accuracy of 10–15%.

B. Experimental Results

The inelastic magnetic scattering was investigated mainly in the neutron-energy-loss mode at temperatures between 1.9 and 40 °K. The results are best described by considering first the low-temperature data, and then the scattering observed at higher temperatures. Before describing the results at finite $\vec{q}$ we discuss the region around $q_{c^*} = 0$, where anomalous scattering is observed.

1. *Difficulties at Low q_{c^*}*

In the region around $\omega = 0$ a contribution from nuclear incoherent scattering is always present. A typical scan at 4.4 °K at the position (0.2, 0, 1.05) which corresponds to $q_{c^*} = 0.05$ is shown in Fig. 5. The peak in the center arises entirely, within experimental errors, from the nuclear incoherent scattering; it is found to be essentially independent of $\vec{Q}$ for $|q_{c^*}| \geq 0.05$ in the general region (0.2, 0, 1). The full width at half-maximum (FWHM) is ~0.6 meV. The satellite peaks are the spin waves which we shall discuss extensively in Sec. V B 2.

At $q_{c^*} \sim 0$, however, additional anomalous scattering peaks are observed; typical examples are given in Fig. 6. These peaks are present at both nuclear and magnetic planes (unlike the spin waves) and it appears that they are almost independent of temperature. This would seem to necessitate that they are nuclear in origin. The peaks vary in energy and intensity with the incident neutron energy and the value of $\hbar$ at which they are observed on the plane. They are also seen at small values of $q_{c^*} \neq 0$, but in all cases they only occur when the half-intensity contour of the resolution ellipsoid encompasses the point $q_{c^*} = 0$, $\omega = 0$, and they generally appear with much smaller FWHM than the incoherent scattering. Finally, they have no apparent symmetry about $q_{c^*} = 0$ or $\omega = 0$.

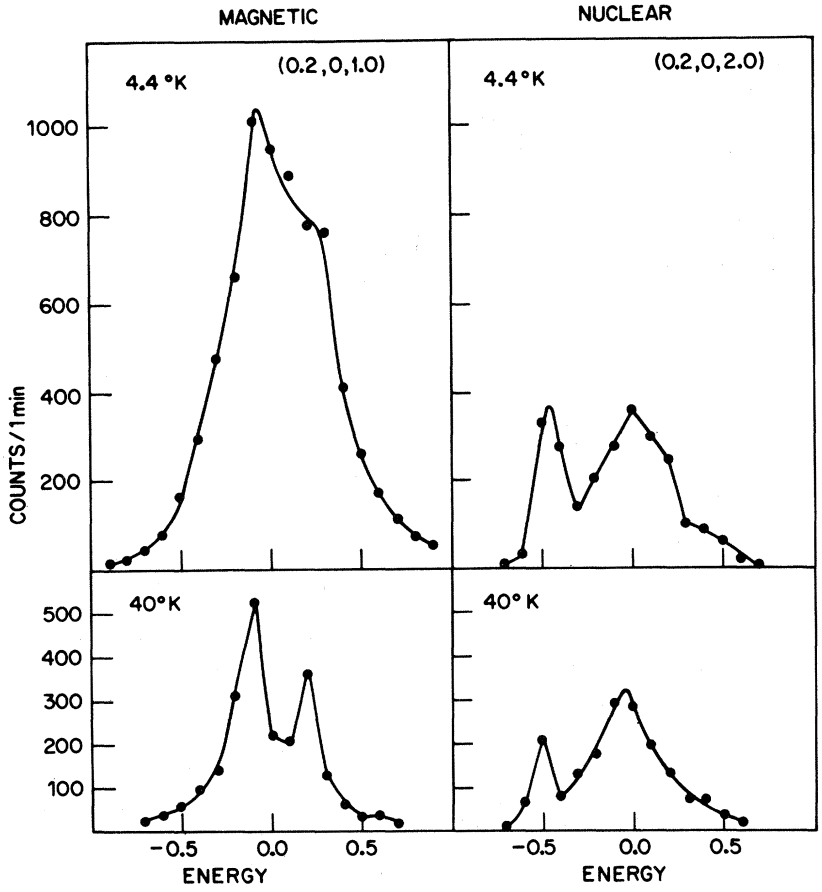

FIG. 6. Typical energy scans exhibiting anomalous peaks at the magnetic and nuclear integer plane positions (0.2, 0, 1), (0.2, 0, 2).

The magnetic contribution at the $l = 1$ plane can be clearly seen from Fig. 6, where there is a large difference in the scattering intensity observed at 4.4 and 40 °K. However, until the origin of the anomalous peaks is fully established we cannot make any quantitative statements about the magnetic scattering in this region. In particular, we can make no statement about the existence of very long-wavelength spin waves at low temperatures.

2. *Low-Temperature Scattering*

The inelastic scattering corresponding to momentum transfers greater than about 0.04 reciprocal-lattice units is found to have a very simple form at 1.9 °K. Constant-Q scans made relative to the $l = 1$ plane show that the only appreciable scattering above background occurs in the form of sharp peaks with widths determined by the instrumental resolution function. Typical scans as a function of wave vector are shown in Fig. 7; these cover wave vectors ranging from $q_{c*} = 0.05$ to 0.25, that is, halfway to the zone boundary. When the temperature is increased to 4.4 °K the peaks are found to decrease slightly in height and to broaden slightly, but there is no measurable change in the peak positions. Figure 8 shows typical scans at 4.4 °K covering wave vectors ranging between $q_{c*} = 0.1$ and 0.5, the zone-boundary position.

The dispersion relation for these excitations is shown in Fig. 9. In the $\vec{c}^*$ direction the fitted dispersion follows a perfect sine curve, passing through the origin within the experimental error. Furthermore, for fixed q_{c*}, the energy of the peak intensity is independent of q_{a*}, the momentum component perpendicular to the $MnCl_3$ chains. It is clear that these excitations are simply 1d spin waves which propagate along individual $MnCl_3$ chains. It is of interest to compare the observed scattering directly with that predicted from the spin-wave theory for $S^{xx}(\vec{Q}, \omega)$ given in Eqs. (8)–(11). The theory involves just two adjustable parameters, an effective exchange constant $(J_{nn} - 2J_{nnn})R$, and an over-all scaling factor for the intensities. The solid lines in Figs. 7 and 8 are theoretical line shapes obtained from a best fit of the spin-wave theory to the peak positions and heights. At 1.9 °K the agreement between experiment and theory is remarkably good; the positions, intensities, and widths of all the peaks are correctly accounted for. That is, simple spin-wave theory fully accounts for both the eigenvalues and eigenfunctions of the excitations for $q_{c*} \geq 0.05$ at 1.9 °K.

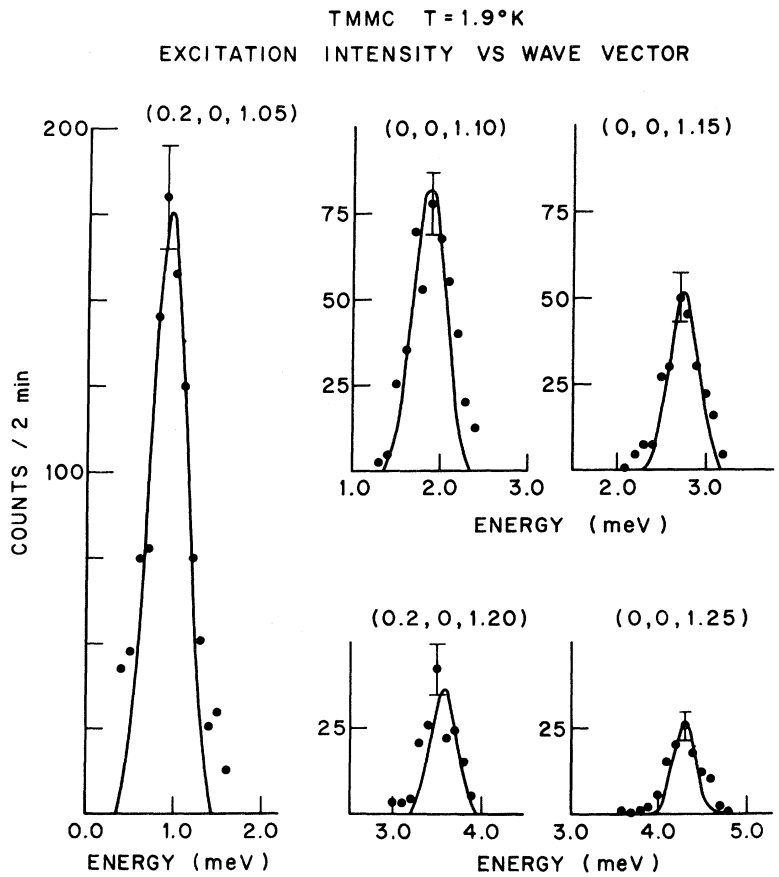

FIG. 7. Excitations in TMMC at 1.9 °K as a function of reduced wave vector q_{c*}. The points are experimental counts with single standard-deviation errors; all counts have been normalized to the same scale. The solid lines are theoretical curves calculated by convoluting the instrumental resolution function with the single-spin-wave-scattering cross section, Eq. (8), using a best-fit normalization.

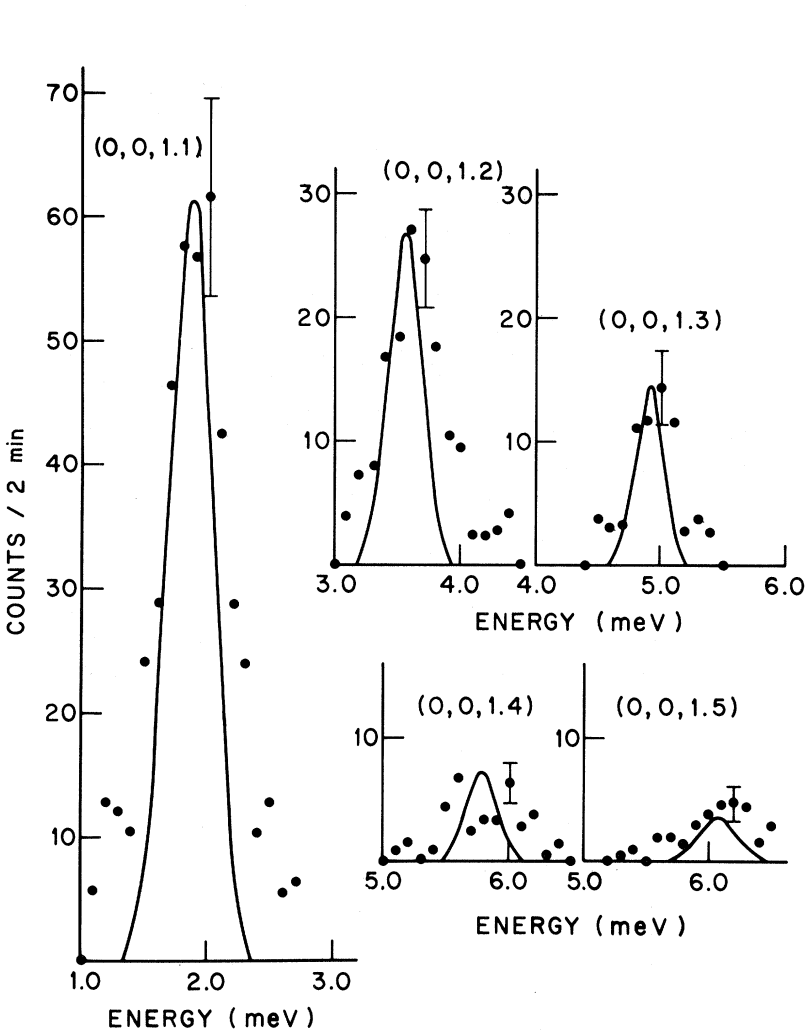

FIG. 8. Excitations in TMMC at 4.4 °K as a function of reduced wave vector q_c*. The points are experimental counts with single standard-deviation errors; all counts have been normalized to the same scale. The solid lines are theoretical curves calculated by convoluting the instrumental resolution function with the single-spin-wave-scattering cross section, Eq. (8), using a best-fit normalization.

At 4.4 °K the agreement is again satisfactory although in this case the widths are not completely accounted for on the basis of the instrumental resolution function alone. The exchange parameter describing the theoretical dispersion relation in Fig. 9 is

$$R(J_{nn} - 2J_{nnn}) = (-0.610 \pm 0.005)\ \text{meV}$$
$$= (-7.07 \pm 0.06)\ ^\circ\text{K}\ .$$

An interesting feature of the scattering observed just above T_N in the 3d Heisenberg antiferromagnet $RbMnF_3$ is the existence of a three-peaked structure in typical constant-Q scans away from the superlattice position.[1] Here the central peak is the tail of the diffusive critical mode, and the satellite peaks are thought to be paramagnetic spin waves. In the 1d paramagnet as we have seen above, the satellite peaks are the dominant feature of the scattering. It is clearly important to determine if there is also a central component in this case. As we have mentioned previously, the region around $\omega = 0$ is complicated by the large nuclear incoherent scattering. However, this incoherent scattering can be determined accurately from scans made at a number of positions near the zone boundary, averaging the resulting intensity near $\omega = 0$. Figure 5 shows the theoretical line shape at 4.4 °K at q_c* = 0.05 calculated assuming a spin-wave contribution together with the nuclear incoherent scattering. The spin-wave contribution was determined from the corresponding data at 1.9 °K at larger q_c* while the nuclear incoherent scattering was determined as described above. The solid line in Fig. 5 therefore involves no adjustable parameters; it is evident that all of the scattering is fully accounted for within

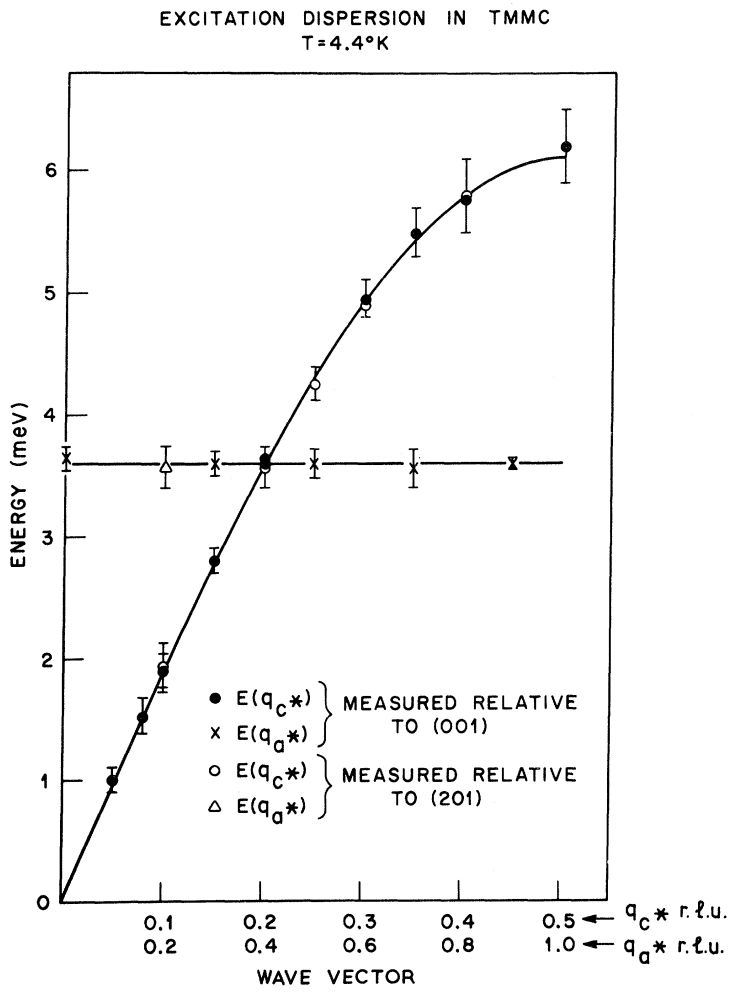

FIG. 9. Dispersion of the excitations in TMMC at 4.4 °K. The experimental points with circles show dispersion in the c^* direction. The other points show the dispersion in the a^* direction at $q_{c^*} = 0.2$ reciprocal-lattice units. The errors represent single standard deviations. The solid-line curve is the best fit to the c^* dispersion. q_{c^*} and q_{a^*} are in reciprocal-lattice units, $2\pi/c$ and $4\pi/\sqrt{3}a$.

the statistical errors. Indeed if there is any central component arising from the magnetic fluctuations then it must have a peak intensity less than 20% of that of the neutron-energy-loss spin wave. This same conclusion is found to hold for larger q_{c^*} although usually with less statistical confidence.

A final aspect of the low-temperature data which is of theoretical importance is the dependence of the scattering on the angle between $\vec{Q}$ and the chain axis. In particular, we should like to know whether or not $S^{\alpha\alpha}(\vec{Q}, \omega)$ has Heisenberg (isotropic) symmetry or if only the components perpendicular to the preferred spin axis are finite. No extensive study of this point was made but scans were carried out at (0. 0, 0, q_{c^*}) and (2. 2, 0, q_{c^*}) for several values of q_{c^*}. In all cases the relative intensities could be accounted for on the basis of the form factor alone, indicating no geometrical effects. However, the statistical confidence of this result is rather low.

3. *Temperature Variation of Excitations*

Measurements of the temperature variation of these excitations were made at three values of wave vector $q_{c^*} = 0.05$, 0. 10, and 0. 25, and the results are shown in Figs. 10–12. An incident energy of 14. 8 meV was again used. The nuclear incoherent scattering has been subtracted in these figures using measurements of its intensity made in the region of the zone boundary.

As the temperature is raised, the excitations broaden. The scattering increases on the low-energy side, corresponding to a decrease in the second moment of the energy-loss spectrum. However, there is no observable shift in the position of the peaks, nor in that of their high-energy cutoff. There is also little variation in width with q_{c^*} at fixed temperature. One notable feature is the persistence of well-defined excitations above the temperature at which the correlation length falls below the wavelength of the excitations. Thus at $q_{c^*} = 0.05$, $\lambda = 128$ Å, well-defined excitations are observed at 12 °K where $\xi \sim 35$ Å; and at $q_{c^*} = 0.1$, $\lambda = 64$ Å, excitations are observed at 20 °K where $\xi \sim 22$ Å. At $q_{c^*} = 0.25$, $\lambda = 25$ Å, it is still possible to see a broad peak at 40 °K corresponding to ξ

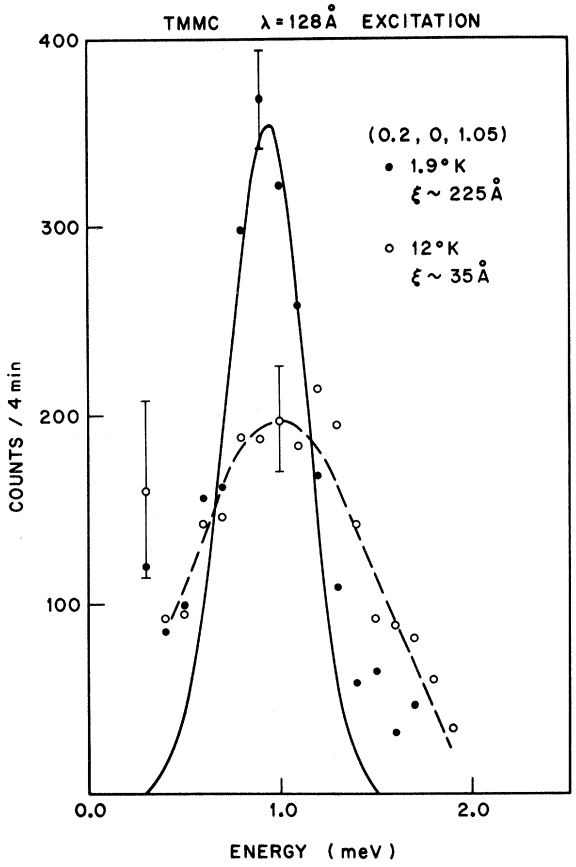

FIG. 10. Variation with temperature of the excitation at (0.2, 0, 1.05), $q_c^* = 0.05$ reciprocal-lattice units. The solid line is calculated, as in Fig. 7.

~9 Å.

There is at the present time no theory with which to compare these experimental results so we must confine ourselves to qualitative statements only; we do this in Sec. VI.

VI. DISCUSSION AND CONCLUSIONS

The outstanding feature of the dynamical behavior of the spins in TMMC is the apparently remarkable result that long-lived 1d spin-wave-like excitations are observed over most of the Brillouin zone at low temperatures. Furthermore, simple two-sublattice spin-wave theory appears to account fully for both the position and relative intensities of the observed neutron groups. This result is perhaps not quite so surprising as it might first appear in view of the exact solution of des Cloiseaux and Pearson for the first excited states of the $S = \frac{1}{2}$ Heisenberg antiferromagnet at absolute zero. From the work of Bonner and Fisher[44] and others[45] we know that this system shows no long-range order, yet the first excited states are found to follow a simple sine-wave dispersion curve differing by only a multiplying factor

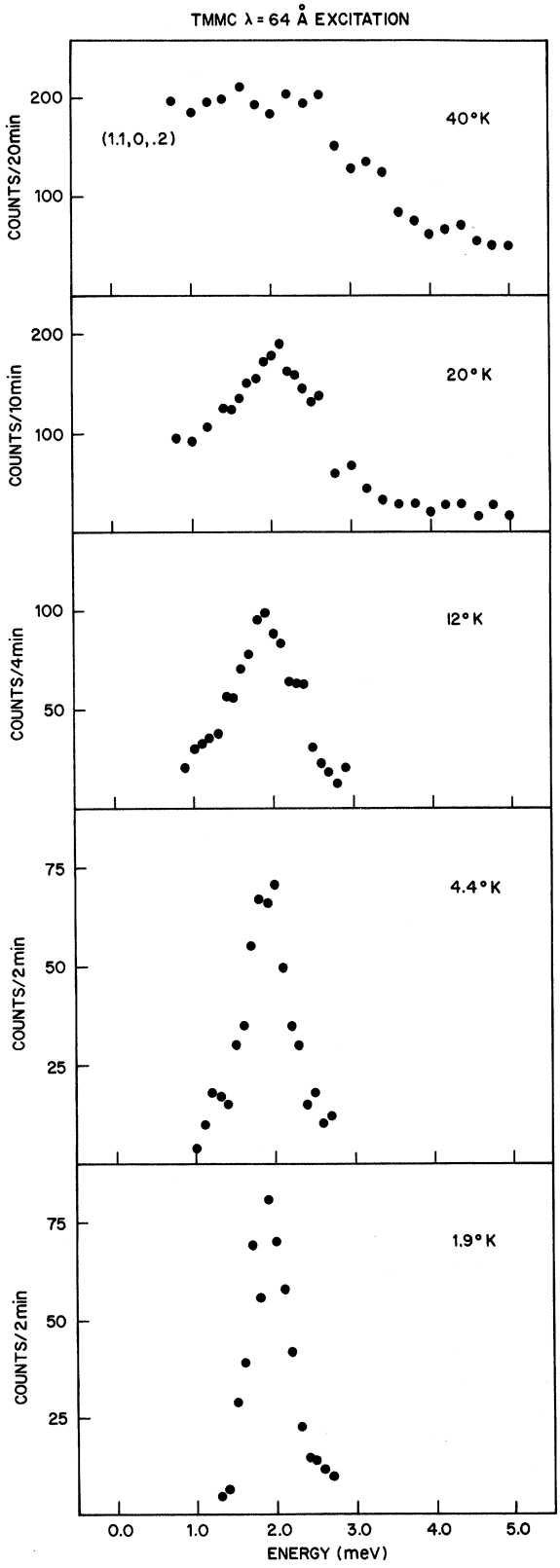

FIG. 11. Variation with temperature of the excitation at (0.2, 0, 1.10), $q_c^* = 0.10$ reciprocal-lattice units.

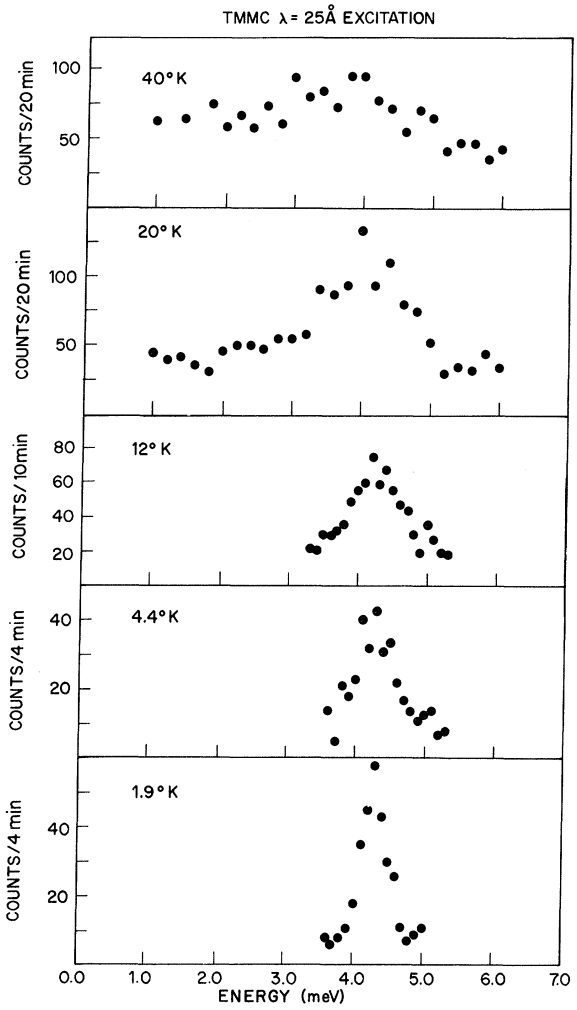

FIG. 12. Variation with temperature of the excitation at $(0.2, 0, 1.25)$, $q_{c*} = 0.25$ reciprocal-lattice units.

from that given by two-sublattice spin-wave theory. One might expect the Néel state, and therefore two-sublattice spin-wave theory, to be a better approximation for a $S = \frac{5}{2}$ system at very low temperatures.

One simple physical picture of paramagnetic spin waves is that based on the concept of short-wavelength spin waves propagating within regions of slowly varying correlated spins.[46] The time variation of the z component of the spins in these correlated regions gives rise to a diffusive peak in $\mathcal{S}(\vec{Q}, \omega)$ centered at $\omega = 0$, the spin waves giving rise to satellite peaks. As we have seen, we are unable to detect the presence of any central peak in TMMC because of the incoherent scattering, but we do know that it is certainly much weaker than the spin-wave peaks. On this model the long-wavelength excitations would be expected to weaken and broaden as the temperature is raised, both because of the decrease in correlation length and because of the thermal population of similar states which may then interact. At 1.9 °K, the correlation length $\xi \sim 210$ Å, so that the longest-wavelength spin waves we observed might indeed be expected to be sharp. It would clearly be interesting to investigate the nature of the very long-wavelength excitations in the region of smaller q, inaccessible to neutrons, at this temperature.

When the temperature is raised, however, the observed spin waves broaden more slowly than the above model would seem to predict. As we have seen, well-defined excitations are observed at each of the temperatures 12, 20, and 40 °K at wavelengths where it is only possible to fit about one-third of a wavelength into a region of correlated spins, that is, $\lambda \sim 3\xi$. On the other hand, if we consider the behavior in terms of the excitation wave vector $q = 2\pi/\lambda$ and $\kappa = \xi^{-1}$, these peaks are still in the regime of $q \gtrsim \kappa$. There may well be more theoretical significance in this latter comparison rather than the former simple physical picture, but a detailed explanation must clearly await a complete calculation from first principles. The recent work of McClean and Blume[20] and of Blume, Vineyard, and Watson[21] appears likely to help to account for the temperature variation of the scattering.

In deducing a value of the exchange constant J_{nn} from the spin-wave dispersion at low temperatures, we must make the assumption, also made in the analysis of the static susceptibility and the quasi-elastic neutron scattering, that the next-nearest-neighbor interaction J_{nnn} is negligible. From the dispersion we find no evidence for a finite value of J_{nnn}, but as we have seen, once it is very small, it cannot be detected from $E(q_{c*})$ alone. However, as the next-nearest-neighbor interaction involves three intervening ions Cl-Mn-Cl, it is likely to be very small, and in other compounds ions separated in a similar manner are found to be very weakly interacting.[47] The assumption therefore appears to be quite reasonable.

Although the determination of exchange constants in an ordered antiferromagnet is best accomplished by a detailed analysis of the spin-wave spectrum, care must clearly be taken in the present case of a 1d paramagnet because of the lack of fundamental justification for the use of spin-wave theory. From our data we have found that $RJ_{nn} = (-7.07 \pm 0.06)$ °K, and we have seen that both Oguchi's or Davis's first-term correction to linear spin-wave theory, and Weng and Griffiths's formula, indicate $R \sim 1.07$–1.08 and therefore $J_{nn} = -(6.6 \pm 0.15)$ °K. This compares favorably with the value of $J_{nn} = (-6.47 \pm 0.13)$ °K found from the analysis of the static susceptibility in terms of Rushbrooke and Woods's exact series expansion. However, until a complete theory is available we can only take this as indicating that the correction factor R is likely to be of

the order of that estimated by these approximate theories. We must also bear in mind the much larger value of $J_{nn} = (-7.7 \pm 0.3)\,^{\circ}\mathrm{K}$ found from the quasielastic scattering; at present we have no explanation for its difference from the value found from the static susceptibility.

The theoretical relationship between the present data on the spin dynamics, and those on the quasielastic scattering, is not as straightforward as expected. The dynamical behavior of the spins at low temperatures is quite definitely quantum mechanical rather than classical in nature, as is evident from Fig. 5, for example, where it may be seen that the relative intensities for magnon creation and annihilation are consistent with Bose statistics and the fact that $\hbar\omega > k_B T$. We would therefore expect $S(\vec{q}) = \int S(\vec{Q}, \omega)\, d\omega$ to follow a $1/q_{c*}$ variation at this temperature. However, the quasielastic-scattering data are consistent with a classical model for which $\hbar\omega \ll k_B T$, and where for $q_{c*} \gg \kappa$, $S(\vec{q}_{c*}) \sim 1/q_{c*}^2$. As the quasielastic scattering is dominated by the slow long-wavelength fluctuations it seems reasonable that classical theory should hold at the higher temperatures. To resolve the above discrepancy we must suppose that either the classical model for $S(\vec{q}_{c*})$ must break down in the region $q_{c*} \gg \kappa$, or there must be an extra contribution to $S(\vec{Q}, \omega)$ in addition to that of the spin waves. Unfortunately, we cannot test these ideas experimentally since the quasielastic scattering is generally too weak in that region of q_{c*} where well-defined spin waves are observed.

Finally we should note that our experiments have not cast any light on the nature of the two-magnon scattering in TMMC. In particular we do not observe any anomalous effects which can be directly attributed to the two-spin part of $S^{zz}(\vec{Q}, \omega)$. An experiment using polarized neutrons would thus be of considerable interest in elucidating the nature of the scattering, which as far as we can tell is isotropic in character. We have also not detected any evidence of bound states in this system.

In conclusion, both the static and dynamic spin fluctuations in TMMC appear to have a simple form which, at low temperatures at least, can be understood using simple physical ideas and existing theory. The thermal development of the dynamic fluctuations has yet to be accounted for. It is hoped that these results will stimulate efforts towards a fundamental theory of magnetism in 1d systems at finite temperatures.

ACKNOWLEDGMENTS

We wish to acknowledge helpful discussions with M. Blume, W. F. Brinkman, M. E. Fisher, B. I. Halperin, P. C. Hohenberg, M. E. Lines, P. C. Martin, F. B. McClean, and J. Skalyo, Jr. We should also like to thank P. C. Hohenberg for a critical reading of the manuscript.

---

*Present address: A.E.R.E., Harwell, Didcot, Berks, England.

†Work performed under the auspices of the United States Atomic Energy Commission.

‡Guest scientist at Brookhaven National Laboratory, Upton, New York.

[1]R. Nathans, F. Menzinger, and S. J. Pickart, J. Appl. Phys. 39, 1237 (1968).

[2]C. G. Windsor, G. A. Briggs, and M. Kestigan, J. Phys. C 1, 940 (1968).

[3]H. Y. Lau, L. M. Corliss, A. Delapalme, J. M. Hastings, R. Nathans, and A. Tucciarone, Phys. Rev. Letters 23, 1225 (1969); J. Appl. Phys. 41, 1384 (1970).

[4]A. Tucciarone, J. M. Hastings, and L. M. Corliss, Phys. Rev. Letters 26, 257 (1971).

[5]M. T. Evans and C. G. Windsor, J. Phys. Suppl. 32, C1-614 (1971).

[6]G. F. Reiter, Solid State Commun. 7, 1327 (1967).

[7]M. Blume and J. Hubbard, Phys. Rev. B 1, 3815 (1970); J. Hubbard, J. Phys. C 4, 53 (1971).

[8]B. I. Halperin and P. C. Hohenberg, Phys. Rev. 177, 952 (1969).

[9]B. I. Halperin and P. C. Hohenberg, Phys. Rev. 188, 898 (1969).

[10]J. Skalyo, Jr., G. Shirane, R. J. Birgeneau, and H. J. Guggenheim, Phys. Rev. Letters 23, 1394 (1969).

[11]J. Skalyo, Jr., G. Shirane, S. A. Friedberg, and H. Kobayashi, Phys. Rev. B 2, 4632 (1970).

[12]See, for example, L. D. Landau and E. M. Lifshitz, *Statistical Physics* (Pergamon, London, 1964), p. 482.

[13]A preliminary account of this work was given at the Sixteenth Conference on Magnetism and Magnetic Materials [M. T. Hutchings, G. Shirane, R. J. Birgeneau, R. Dingle, and S. L. Holt, J. Appl. Phys. 42, 1265 (1971)].

[14]R. Dingle, M. E. Lines, and S. L. Holt, Phys. Rev. 187, 643 (1969).

[15]R. J. Birgeneau, R. Dingle, M. T. Hutchings, G. Shirane, and S. L. Holt, Phys. Rev. Letters 26, 718 (1971).

[16]M. E. Fisher, Am. J. Phys. 32, 343 (1964). See also H. E. Stanley, Phys. Rev. 179, 570 (1969).

[17]E. Lieb, T. Schultz, and D. C. Mattis, Ann. Phys. (N.Y.) 16, 407 (1961).

[18]J. des Cloizeaux and J. J. Pearson, Phys. Rev. 128, 2131 (1962). See also A. A. Ouchinnikov, Zh. Eksperim. i Teor. Fiz. 56, 1354 (1969) [Sov. Phys. JETP 29, 727 (1969)].

[19]J. des Cloizeaux and M. Gaudin, J. Math. Phys. 7, 1384 (1966).

[20]F. B. McClean and M. Blume, J. Appl. Phys. 42, 1380 (1971).

[21]M. Blume, R. E. Watson, and G. H. Vineyard, Bull. Am. Phys. Soc. B16, 629 (1971).

[22]P. M. Richards and F. Carboni, following paper, Phys. Rev. B 5, 2014 (1972).

[23]See, for example, F. Carboni and P. M. Richards, Phys. Rev. 177, 889 (1969); J. F. Fernandez and H. A. Gersch, *ibid.* 172, 341 (1968).

[24]B. Morosin and E. J. Graeber, Acta Cryst. 23, 766 (1967). See also G. D. Stucky, *ibid.* 24, 330 (1968).
[25]R. C. Sherwood (private communication).
[26]G. S. Rushbrooke and P. J. Wood, J. Mol. Phys. 1, 257 (1958).
[27]See, for example, R. J. Birgeneau, M. T. Hutchings, and W. P. Wolf, Phys. Rev. Letters 17, 308 (1966).
[28]R. E. Dietz, F. R. Merritt, R. Dingle, D. Hone, R. G. Silbernagel, and P. M. Richards, Phys. Rev. Letters 26, 1186 (1971).
[29]T. Smith and S. A. Friedberg, Phys. Rev. 176, 660 (1968).
[30]W. Marshall and R. D. Lowde, Rept. Progr. Phys. 31, 705 (1968).
[31]P. W. Anderson, Phys. Rev. 86, 694 (1952).
[32]For a review of spin-wave theory in antiferromagnets see F. Keffer, in *Handbuch der Physik*, edited by S. Flügge (Springer-Verlag, Berlin, 1966), Vol. 18, Pt. 2, p. 1.
[33]O. Nagai and A. Yoshimori, Progr. Theoret. Phys. (Kyoto) 25, 595 (1961).
[34]T. Oguchi, Phys. Rev. 117, 117 (1960).
[35]H. L. Davis, Phys. Rev. 120, 789 (1960).
[36]C.-Y Weng and R. B. Griffiths (private communication).
[37]R. A. Cowley, W. L. J. Buyers, P. Martel, and R. W. H. Stevenson, Phys. Rev. Letters 23, 86 (1969).
[38]D. C. Mattis, *The Theory of Magnetism* (Harper and Row, New York, 1965), Chap. 6.
[39]See M. P. Schulhof, R. Nathans, P. Heller, and A. Linz, Phys. Rev. B 4, 2254 (1971), and references therein.
[40]T. Riste, Nucl. Instr. Methods 86, 1 (1970); and A. C. Nunes and G. Shirane, *ibid.* 95, 445 (1971).
[41]G. Shirane and V. J. Minkiewicz, Nucl. Instr. Methods 89, 109 (1970).
[42]M. J. Cooper and R. Nathans, Acta Cryst. 23, 357 (1967).
[43]The program is discussed by E. J. Samuelsen, in *Structural Phase Transitions and Soft Modes* (NATO Advanced Study Institute, Geilo, Norway, to be published).
[44]J. C. Bonner and M. E. Fisher, Phys. Rev. 135, A640 (1964).
[45]E. H. Lieb and D. C. Mattis, *Mathematical Physics in One Dimension* (Academic, New York, 1966), Chap. 6.
[46]See, for example, W. Marshall, Natl. Bur. Std. (U.S.) Misc. Publ. 273, 135 (1966).
[47]For example, see O. Nikotin, P. A. Lindgard, and O. W. Dietrich, J. Phys. C 2, 1168 (1969).

PHYSICAL REVIEW B VOLUME 5, NUMBER 5 1 MARCH 1972

Spin Waves in Finite Spin-$\frac{1}{2}$ Heisenberg Chains*

Peter M. Richards
Department of Physics, University of Kansas, Lawrence, Kansas 66044

and

Fernando Carboni
Department of Physics, Universidad de Oriente, Cumana, Venezuela

(Received 2 June 1971)

Previously unpublished calculations of Carboni and Richards are compared with inelastic-neutron-scattering data in $(CH_3)_4NMnCl_3$ (TMMC). The calculations, which are exact for frequency and temperature dependence of two spin-correlation functions in spin-$\frac{1}{2}$ antiferromagnetic Heisenberg chains containing up to nine spins, show a spin-wave peak at low temperature. The peak broadens and disappears at higher temperatures but does not show an appreciable energy renormalization. These features are consistent with neutron observations of spin waves in TMMC.

I. INTRODUCTION

Neutron scattering has demonstrated[1] the existence of antiferromagnetic spin-wave modes in the linear-chain compound $(CH_3)_4NMnCl_3$ (referred to as TMMC). They are well defined at temperatures up to near 40 °K, compared with a classical zone-boundary magnon energy of $4JS = 65$ °K. Energy renormalization effects appear to be negligible.

The purpose of this paper is to show that the above features are reproduced in exact calculations for finite chains of spin-$\frac{1}{2}$ particles coupled via the Heisenberg interaction

$$\mathcal{H} = 2J \sum_{i=1}^{N} \vec{S}_i \cdot \vec{S}_{i+1} \,. \tag{1}$$

Some time ago,[2] in a paper referred to as I, we computed time-correlation functions of the form $\langle S_i^x(t) S_j^x \rangle$ by diagonalizing $\mathcal{H}$ for closed chains containing as many as $N = 10$ spins. Since no experimental data existed at that time, we did not reproduce in I correlation functions pertinent to neutron scattering at finite temperatures. Now it is appropriate to document previously unpublished results which point to the existence of spin waves and can be compared with the neutron data.